View metadata, citation and similar papers at core.ac.uk
brought to you by CORE
provided by Repositorio Institucional de la Universidad de Alicante

Coherently Photoinduced Ferromagnetism in Diluted Magnetic Semiconductors

J. Fernández-Rossier,[1,2] C. Piermarocchi,[3,4] P. Chen,[3,5] A. H. MacDonald,[1] and L. J. Sham[3]

[1]*Department of Physics, University of Texas at Austin, University Station C1600, Austin, Texas 78712 USA*
[2]*Departamento de Física Aplicada, Universidad de Alicante, San Vicente del Raspeig 03690, Alicante, Spain*
[3]*Department of Physics, University of California San Diego, 9500 Gilman Drive, La Jolla, California 92093 USA*
[4]*Department of Physics and Astronomy, Michigan State University, 4263 Biomedical and Physical Sciences East Lansing, Michigan 48824-2320 USA*
[5]*Department of Chemistry, University of California Berkeley, 406 Latimer Hall, Berkeley, California 94720-1460 USA*

(Received 19 December 2003; published 14 September 2004)

Ferromagnetism is predicted in undoped diluted magnetic semiconductors illuminated by intense *sub-band-gap* laser radiation . The mechanism for photoinduced ferromagnetism is coherence between conduction and valence bands induced by the light which leads to an optical exchange interaction. The ferromagnetic critical temperature T_C depends both on the properties of the material and on the frequency and intensity of the laser and could be above 1K.

DOI: 10.1103/PhysRevLett.93.127201 PACS numbers: 75.50.Pp

Information processing in electronic devices is based on control of charge flow in semiconductor materials, whereas nonvolatile information storage exploits ferromagnetism, spontaneous alignment of the spins of many electrons. *Spintronics* [1] aims to achieve a merger of these technologies, motivating interest in new ferromagnetic semiconductors like (Ga,Mn)As and other (III,Mn)V compounds [2] and in diluted magnetic semiconductors (DMS) like (Cd,Mn)Te and other (II,Mn)VI materials [3] with free moments that can be aligned by external fields. The optical properties of these semiconductors are particularly interesting in this respect because laser radiation can control both charge and spin dynamics[4].

In this Letter we predict a qualitatively new effect, photoinduced ferromagnetism, in which magnetic order is induced in an otherwise paramagnetic (II,Mn)VI DMS by laser light that is *below* the absorption edge. The influence of the laser field on the electronic system is reactive, rather than dissipative, and follows ultimately from a change in the effective electronic Hamiltonian analogous to those that yield dipole forces in atomic physics. The II–VI parent compounds are intrinsic semiconductors with states of p character at the top of the valence band and of s character at the bottom of the conduction band [5]. They have a sizable interband optical matrix element, $\vec{d}_{cv} = \langle v|e\vec{r}|c\rangle$. In (II,Mn)VI alloys, Mn substitutes for the group-II atoms. The electronic structure of the external s, p shells of Mn and group-II atoms is very similar, so that the conduction and valence band are barely affected by moderate Mn doping. However, the d shell of each Mn atom is only half full, in contrast to the full shells of the atoms for which they substitute, and forms a local moment with spin $S = \frac{5}{2}$. These magnetic moments are the only low energy electronic degrees of freedom in ideal (II,Mn)VI materials.

The magnetic moment of a Mn d shell interacts with the spins of electrons in both conduction and valence bands through the exchange coupling

$$\mathcal{H}_{\text{exch}} = \sum_{i,b} J_b \vec{M}_i \cdot \vec{S}_b(\vec{R}_i), \tag{1}$$

where $\vec{M}_i$ refers to the Mn atom located at $\vec{R}_i$, the spin density of the $b = e$ conduction electrons and $b = h$ valence band holes is $\vec{S}_b(\vec{R}_i)$, and J_b are the exchange coupling constants [5]. When the Mn atoms are spin-polarized, this interaction leads, in a mean field and virtual crystal approximation whose approximate validity is well established [5,6], to an effective magnetic field $g\mu_B \vec{B}^{\text{eff}} \equiv J_{e,h} c_{\text{Mn}} \vec{\mathcal{M}}$ experienced by the spins of the carriers, where c_{Mn} is the density of Mn atoms and $\vec{\mathcal{M}}$ is their average magnetization.

In doped systems, band electrons mediate RKKY interactions between Mn spins. On the other hand, virtual fluctuations in the Mn valence lead to short range superexchange antiferromagnetic interactions which couple only nearest neighbors. In a sample with a fraction x of Mn randomly located at the cation sites, $x_{\text{eff}} \equiv x(1-x)^{12}$ is the fraction of sites containing Mn atoms without a magnetic first neighbor. Consequently, samples with a low Mn concentration ($x \simeq 0.01$) and no band carriers are paramagnetic. It has been shown [7] that two localized spins in a semiconductor can interact via the virtual carriers created in the (otherwise empty) bands by a laser of frequency smaller than the band gap. The effective interaction is a ferromagnetic Heisenberg coupling which we shall call optical RKKY. It is our contention that the optical RKKY interaction can drive a diluted magnetic semiconductor into a ferromagnetic phase at low temperatures.

When the material is illuminated by a laser with electric field E_α and frequency ω_L below the semiconductor band gap E_g, a reactive dipolar energy is stored in the semiconductor:

 © 2004 The American Physical Society

$$\mathcal{E} = -\sum_{\alpha\beta} \chi'_{\alpha\beta}(\omega_L) E_\alpha E_\beta \tag{2}$$

where $\chi'_{\alpha\beta}(\omega_L)$ is the real part of the retarded optical response function. In this case the laser field acts like a new tunable thermodynamic variable which changes the properties of the system. $\chi'_{\alpha\beta}(\omega)$ depends on the interband transition energies which, due to the exchange interaction (1), depend in turn on the collective magnetization $\vec{\mathcal{M}}$. In an illuminated sample, $\mathcal{E}$ *does* depend on $\vec{\mathcal{M}}$. As we show below, $\mathcal{E}$ is minimized when the Mn spins are fully polarized and the system is ferromagnetic. Importantly, because $\hbar\omega_L < E_g$, the dissipative part $\chi''_{\alpha\beta}(\omega_L)$ of the response function is zero, so that no real electron-hole pairs are created, and heating is strongly suppressed.

We now derive $\mathcal{E}$ starting from the microscopic Hamiltonian. The relevant degrees of freedom are the electrons in the conduction band, holes in the valence band, and the Mn spins. The exchange interaction (1) is included in the mean field and virtual crystal approximation, which results in a spin splitting of the bands when the Mn spins are polarized [5,6]. For simplicity, we have neglected the important spin-orbit interaction influence on the valence bands. A classical laser field couples the valence and conduction bands. We only consider here the case of unpolarized laser light, where the two optically active interband transitions are driven with equal strength. We use the selection rule for the heavy holes at $k = 0$ so that an electron with spin σ is promoted from the valence band to the conduction band. The resultant magnetization comes from the cooperative effects of the Mn spins through their interactions with the carriers, unlike optical orientation effects that can be induced by polarized light in these materials.

The Hamiltonian reads $H = H_c + H_v + H_L + V_C$ with:

$$\begin{aligned}
H_c &= \sum_{\sigma,\vec{k}} \left[\epsilon^e_{\vec{k}} - \frac{\sigma}{2} J_e c_{Mn} |\vec{\mathcal{M}}| \right] c^\dagger_{\vec{k},\sigma} c_{\vec{k},\sigma}, \\
H_v &= \sum_{\sigma,\vec{k}} \left[\epsilon^h_{\vec{k}} - \frac{\sigma}{2} J_h c_{Mn} |\vec{\mathcal{M}}| \right] d^\dagger_{\vec{k},\sigma} d_{\vec{k},\sigma}, \\
H_L &= \frac{\Omega}{2} \sum c^\dagger_{\vec{k},\sigma} e^{i\omega_L t} d^\dagger_{\vec{k},\sigma} + h.c., \\
V_C &= \frac{1}{2\mathcal{V}} \sum_{\vec{q}} V(\vec{q}) \rho(\vec{q}) \rho(-\vec{q})
\end{aligned} \tag{3}$$

where we have chosen the spin quantization axis along the collective magnetization axis $\vec{\mathcal{M}}$. The conduction and valence band dispersions are $\epsilon^e_{\vec{k}}$ and $\epsilon^h_{\vec{k}}$ respectively. The strength of the light matter coupling is quantified by the Rabi energy, $\Omega = d_{cv} E_0$, where E_0 is the amplitude of the electric field of the laser. The last term accounts for the Coulomb interaction in the dominant term approximation with $\rho(q) = \rho_e(q) - \rho_h(q)$, $\rho_e(q) = \sum_{\vec{k},\sigma} c^\dagger_{\vec{k},\sigma} c_{\vec{k}+\vec{q},\sigma}$, $\rho_h(q) = \sum_{\vec{k},\sigma} d^\dagger_{\vec{k},\sigma} d_{\vec{k}+\vec{q},\sigma}$, $V(q) = \frac{4\pi}{\epsilon q^2}$ and $\mathcal{V}$ stands for the volume of the sample.

The dynamics of the carrier density matrix under the influence of Hamiltonian (3) in the spinless case with $J_{e,h} = 0$ has been studied previously by a number of authors, who treat Coulomb interactions in the Hartree-Fock (HF) approximation [8–10]. Numerical solution of the dynamical equations [10] show that the density matrix reaches a steady state due to the inhomogeneous broadening provided by the different k states. Spontaneous emission and other phenomena will also contribute to the damping of the density matrix dynamics in a time scale T_2 which is in the picosecond range. The HF steady state can be described as the vacuum of a dressed Hamiltonian [9] and resembles very much a BCS state for excitons, where Ω and the electron-hole interaction act as the pairing force, and $\delta_0 \equiv E_g - \omega_L$ plays the role of the chemical potential. When δ_0 is positive and sufficiently large, the average density of band carriers vanishes identically when the laser is switched off. In that limit, the wave function of the ground state of the dressed Hamiltonian can be mapped to a coherent state of noninteracting bosonic excitons [8] with binding energy ϵ_x, Bohr radius a_B, and ground state wave function $\psi_{1s}(r)$ corresponding to the electron-hole Coulomb potential $V(q)$ above.

When the spin degree of freedom is included, the equations for the two optically active channels decouple in the HF approximation [11] for an unpolarized laser. The two sets of equations for the carrier density matrix of the two optically active channels, + and −, are identical to those of the spinless case [8–10] except for the detuning, which acquires a spin dependent magnetic shift. It is useful to define a detuning renormalized by the excitonic effects, $\delta \equiv \delta_0 - \epsilon_x$ and a spin dependent detuning

$$\delta_\pm(\mathcal{M}) = E_g - \omega_L - \epsilon_x \pm J(\mathcal{M}) \equiv \delta \pm J(\mathcal{M}) \tag{4}$$

with $J(\mathcal{M}) \equiv (J_h - J_e) c_{\mathrm{Mn}} \frac{\langle \mathcal{M} \rangle}{2}$. As a result of the magnetization, the detuning in one channel increases, whereas, in the other it decreases. For $\mathcal{M} = 0$ the coherent region (no absorption) occurs for $\delta > 0$ [10]. In order to keep the semiconductor transparent in the ferromagnetic phase, we need $\delta > J(\mathcal{M})$. For the DMS considered below, the magnetic shift is large enough so that the system is in the noninteracting exciton situation for which analytical results are available [8]. For instance, the density of virtual excitons in each channel reads:

$$n_\pm a_B^3 = \frac{1}{4\pi} \frac{\Omega^2}{(\delta_\pm)^2}. \tag{5}$$

This result is valid provided that $n_\sigma a_B^3 < 0.1$, which is the case for all the results presented below. This condition imposes both a lower bound for δ, which must be larger than $\delta_{\min} = |J(\mathcal{M} = S)| = J_{\max}$, and an upper bound for

Ω, which must be smaller than $\Omega_{\max} = 1.12 \times (\delta - \delta_{\min})$. The former is the condition for the material to remain nonabsorbing in the ferromagnetic phase, whereas the latter is the limit for the validity of the independent exciton approximation. In this limit the reactive dipolar energy stored in the semiconductor because of the interaction with the laser reads:

$$\mathcal{E}(\mathcal{M}) = -\frac{\mathcal{V}\Omega^2|\psi_{1s}(0)|^2}{4}\left[\frac{1}{\delta_+} + \frac{1}{\delta_-}\right] \qquad (6)$$

which should be compared with (2). To explore the collective properties of the Mn magnetic moments under the influence of the laser, we assume that the magnetic degrees of freedom are in thermal equilibrium and that their internal energy $\mathcal{E}$ is given by Eq. (6). The magnetization is determined by the competition between the dipolar energy density $\mathcal{G}_\mathcal{E} \equiv \frac{1}{\mathcal{V}}\mathcal{E}(\mathcal{M})$ and the entropy density in $\mathcal{G}_S = -c_{Mn}k_bTS(\mathcal{M})$, where $S(\mathcal{M})$ is the entropy per spin as a function of the magnetization [12]. When the paramagnetic to ferromagnetic phase transition is continuous, we can expand $G(\mathcal{M})$ around $\mathcal{M} = 0$ to obtain an analytical formula for the Curie Temperature:

$$k_BT_C = \frac{S(S+1)}{3}(J_e - J_h)^2 c_{\mathrm{Mn}} \frac{|\psi_{1s}(0)|^2\Omega^2}{4\delta^3}. \qquad (7)$$

We note that the same equation can be derived from the mean field theory using the effective Heisenberg interaction defined by the optical exchange coupling derived in Ref. [7]. From Eq. (7) and the numerical evaluation of T_C shown below, we conclude that the important factors to achieve sizable Curie Temperature are compact excitons (small a_B) and large Rabi energy Ω. From this point of view, (Zn,Mn)S and (Zn,Mn)Se seem to be the most promising in the II–VI family, due to their small Bohr radii.

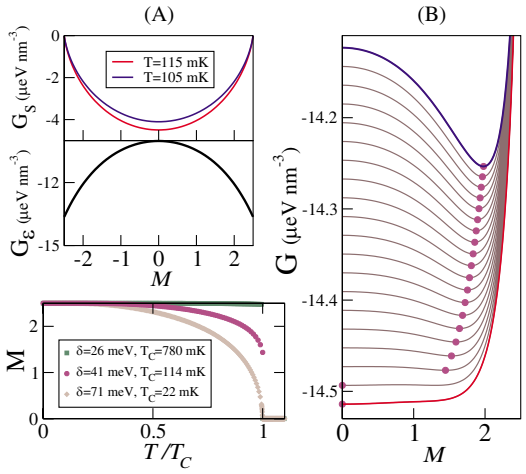

FIG. 1 (color online). Energy contributions as a function of $\mathcal{M}$. (a) Upper panel: $\mathcal{G}_S(\mathcal{M})$ for two different temperatures. Middle panel: $\frac{\mathcal{E}(\mathcal{M})}{\mathcal{V}}$ for $\delta = 41$ meV and $\Omega = 5$ meV. Lower panel: $\mathcal{M}(T/T_c)$ for $\Omega = 5$ meV and three different values of δ. (b) Total Landau energy $\mathcal{G}(\mathcal{M})$ for the Mn, for a set of temperatures nearby T_c for $\delta = 41$ meV and $\Omega = 5$ meV.

In Fig. 1 we plot $\mathcal{G}_\mathcal{E}(\mathcal{M})$ and $\mathcal{G}_S(\mathcal{M})$ for bulk $Zn_{0.988}Mn_{0.012}S$ ($x_{\mathrm{eff}} = 0.01$) under the influence of a laser with Rabi energy $\Omega = 5$ meV and a detuning $\delta = 41$ meV [13]. For this concentration, the magnetic shift for the fully polarized case is $J_{\max} = 21$ meV. The upper panel of Fig. 1(a) shows $\mathcal{G}_S(\mathcal{M})$, which favors magnetic disorder ($\mathcal{M}$=0). In the middle panel of Fig. 1(a) we see how the dipolar energy is minimized for a maximal magnetic order $M = 5/2$. In Fig. 1(b) we plot the total Landau functional $G(\mathcal{M}) = \mathcal{G}_\mathcal{E} + \mathcal{G}_S$ for a set of temperatures between 105 and 115 mK. For each temperature, the order parameter $\mathcal{M}$ is obtained by minimization of $G(\mathcal{M})$ (solid circles in Fig. 1(b)]. The curve $\mathcal{M}(T)$ so generated is shown in the lower panel of Fig. 1(a). A discontinuous phase transition from paramagnetic ($\mathcal{M} = 0$) to ferromagnetic ($\mathcal{M} \neq 0$) occurs at $T_C = 114$ mK. In that panel we also show $\mathcal{M}(T)$ for some other detunings: $\delta = 26$ meV ($T_C = 778$ mK) and $\delta = 71$ meV ($T_C = 22$ mK). We see that T_C is a decreasing function of δ and that the shape of the $\mathcal{M}(T/T_C)$ curve varies; our model predicts continuous and discontinuous phase transitions in different regions of the phase diagram.

The Curie temperature as a function of δ and Ω is shown in Fig. 2(a) for $Zn_{0.988}Mn_{0.012}S$. From Fig. 2(b) it is apparent that ferromagnetism can be switched on and off at a given temperature by adjusting the intensity or the frequency of the laser. For a laser field with Rabi energy $\Omega = 10$ meV and $\delta = 30.5$ meV, our theory predicts $T_C = 1.5$ Kelvin. Continuous wave laser excitation with Rabi splitting $\Omega = 0.2$ meV has been achieved [14] which would yield $T_c \simeq 50$ mK for bulk $Zn_{0.988}Mn_{0.012}S$ and $\delta = 21.6$ meV [15]. It is worth noting that even in the case of [14], in which the detuning is very small and real carrier aborption is enhanced, heating of the sample does not seem to be an issue. Experiments show that specific heat of $(II_{0.99},Mn_{0.01})VI$ is enhanced by a factor of more than 20, at 0.5 K, compared with the parent compound II–VI, because of the magnetic degrees of freedom [16]. This makes the temperature of the magnetic semiconductor more stable than the nonmagnetic parent compound. In strong excitation limit, values of Ω as large as 1.5 eV can be achieved with 5 femtosecond laser pulses [17]. However, in order to observe ferromagnetic order the laser pulse must be longer than the transition switching time, which should presumably have the same order of magnitude as T_1, the Mn longitudinal relaxation time. In the absence of laser driven interactions, this quantity depends strongly on x, the Mn concentration, indicating that the superexchange interactions are the dominant relaxation mechanism [18]. For $x \simeq 0.01$, the laser driven interaction is dominant and presumably as efficient as the superexchange interactions in samples with larger Mn concentrations, where T_1 can be of the order of 0.2 ns [4,18].

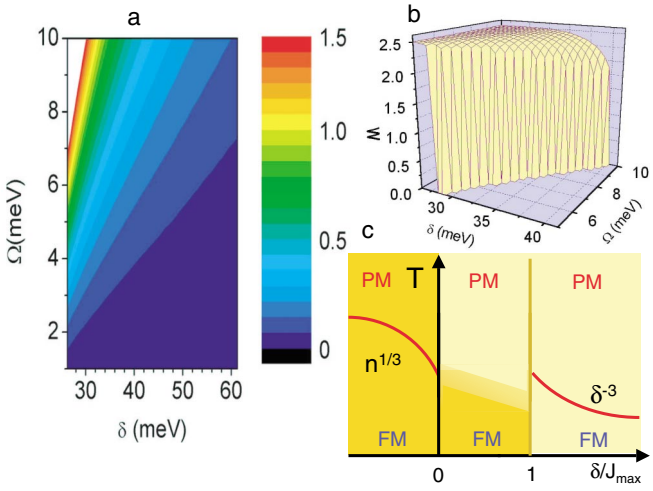

FIG. 2 (color). (a) Contour map for transition temperature as a function of the Rabi energy Ω and the detuning δ, for $(Zn_{0.99}Mn_{0.01})S$. White region: outside validity range of linear response. (b) $\mathcal{M}(\Omega, \delta)$ at a fixed temperature, $k_BT = 0.5$ Kelvin for $Zn_{0.988}Mn_{0.012}S$. (c) Schematic (k_BT, $\delta/J_{\max}$) phase diagram, for fixed laser intensity. In the left region ($\delta < 0$) [right region ($\delta > J_{\max}$)] the system is always absorbing (coherent). The red line in the coherent side signals the ferromagnetic instability described in this work. The red line in the absorbing part corresponds to photocarrier mediated ferromagnetism T_c [6,20]. The middle region shows a possible transition from a paramagnetic-coherent towards a ferromagnetic-absorbing phase.

The full phase diagram in T and δ would have six distinct regimes [see Fig. 2(c)]. For $\delta > J_{\max}$ the semiconductor is always transparent, and the system can undergo the purely coherent ferromagnetic phase transition at a T_C close to the estimates plotted in Fig. 2(a). For $0 < \delta < J_{\max}$, the system is transparent and paramagnetic at high temperature, but has the potential to become ferromagnetic and absorbing at low temperatures. In this situation, the system might return to the paramagnetic phase, because of heating, or might be ferromagnetic (due to the standard RKKY interaction mediated by the real photocarriers). Finally, for negative detuning the system is always absorbing, and photoinduced carriers can lead to ferromagnetism [19] through the same mechanisms that apply for equilibrium carriers, leading to a transition at $k_BT_C = \frac{S(S+1)}{3}\frac{2n^{1/3}c_{\mathrm{Mn}}}{\hbar^2(3\pi^2)^{(2/3)}}(J_{sd}^2 m_c + J_{pd}^2 m_v)$ where n is the density of photocarriers. Ferromagnetism induced by (real) photocarriers has been observed in (Cd,Mn)Te heterostructures at 2 K [20]

In summary, we propose that a diluted magnetic semiconductor exposed to a laser below the absorption threshold will undergo a ferromagnetic phase transition at low temperatures. The ferromagnetism takes place because the reactive dipolar energy induced in the semiconductor is minimized by the ferromagnetic configuration. Microscopically, the spins interact with each other via an optical RKKY interaction mediated by virtual carriers [7]. The ferromagnetic interactions are switched on and off as fast as the laser. The mechanism of this laser induced ferromagnetism relies on interband optical coherence and is radically different from other types of carrier mediated ferromagnetism.

We thank T. Dietl for fruitful discussions. This work has been supported by the Welch Foundation, the Office of Naval Research under grant N000140010951, DARPA/ONR N0014-99-1-1096, NSF DMR 0099572, DMR-0312491, Ministerio de Ciencia y Tecnología, MAT2003-08109-C02-01, and Ramón y Cajal program (MCYT). This has been partly funded by FEDER funds.

[1] S. A. Wolff *et al.*, Science **294**, 1488 (2001).
[2] H. Ohno, Science **281**, 951 (1998); H. Ohno *et al.*, Nature (London) **408**, 944 (2000).
[3] R. Fiederling *et al.*, Nature **402**, 787 (1999).
[4] S. A. Crooker *et al.*, Phys. Rev. B **56**, 7574 (1997); S. Koshihara *et al.*, Phys. Rev. Lett. **78**, 4617 (1997); R. Akimoto *et al.*, Phys. Rev. B **57**, 7208 (1998); A. Gupta *et al.*, Science **292**, 2458 (2001); A. Oiwa *et al.*, Phys. Rev. Lett. **88**, 137202 (2002); J. Wang *et al.*, cond-mat/0305017; J. Bao *et al.*, Nat. Mater. **2**, 175 (2003).
[5] J. K. Furdyna, J. Appl. Phys. **64**, R29 (1988).
[6] T. Dietl *et al.*, Science **287**, 1019 (2000).
[7] C. Piermarocchi *et al.*, Phys. Rev. Lett. **89**, 167402 (2002).
[8] S. Schmitt-Rink, D. S. Chemla, and H. Haug, Phys. Rev. B **37**, 941 (1988).
[9] C. Comte and G. Mahler, Phys. Rev. B **38**, 10517 (1988).
[10] S. Glutsch and R. Zimmermann, Phys. Rev. B **45**, 5857 (1992).
[11] J. Fernández-Rossier and C. Tejedor, Phys. Rev. Lett. **78**, 4809 (1997).
[12] J. Fernández-Rossier and L. J. Sham, Phys. Rev. B **64**, 235323 (2001).
[13] For $Zn_{0.988}Mn_{0.012}S$, we take the exciton Bohr radius $a_B = 21$ Å and the exchange constants $J_e = 7.8$ eV Å^3 ($\alpha = 0.2$ eV) and $J_h = -59.04$ eV Å^3 ($\beta = -1.5$ eV).
[14] H. Kamada *et al.*, Phys. Rev. Lett. **87**, 246401 (2001).
[15] We remark that the experimental values of the Rabi energies mentioned refer to InGaAs/GaAs systems. We are not aware of direct measurements of the Rabi energies in (Zn,Mn)S. However, the dipole transition matrix elements for the two materials are comparable. See, e.g., P. Lawaetz, Phys. Rev. B **4**, 3460 (1971).
[16] R. R. Galazka *et al.*, Phys. Rev. B **22**, 3344 (1980).
[17] O. D. Mücke *et al.*, Phys. Rev. Lett. **87**, 057401 (2001).
[18] T. Dietl *et al.*, Phys. Rev. Lett. **74**, 474 (1995).
[19] E. Pashitsij and S. Ryabchenko, Sov. Phys. Solid State **21**, 322 (1979); Yu. Semenov, Zh. Exp. Teor. Fiz. **81**, 1498 (1981) [Sov. Phys. JETP **54**, 792 (1981)].
[20] H. Boukari *et al.*, Phys. Rev. Lett. **88**, 207204 (2002).